NASA/TM—20250002872

Single-Event Effects Test Report Texas Instruments TDA4VM System on Chip

Edward J. Wyrwas

Scott D. Stansberry

February 2025

NASA STI Program Report Series

The NASA STI Program collects, organizes, provides for archiving, and disseminates NASA's STI. The NASA STI program provides access to the NTRS Registered and its public interface, the NASA Technical Reports Server, thus providing one of the largest collections of aeronautical and space science STI in the world. Results are published in both non-NASA channels and by NASA in the NASA STI Report Series, which includes the following report types:

- TECHNICAL PUBLICATION. Reports of completed research or a major significant phase of research that present the results of NASA Programs and include extensive data or theoretical analysis. Includes compilations of significant scientific and technical data and information deemed to be of continuing reference value. NASA counterpart of peer-reviewed formal professional papers but has less stringent limitations on manuscript length and extent of graphic presentations.

- TECHNICAL MEMORANDUM. Scientific and technical findings that are preliminary or of specialized interest, e.g., quick release reports, working papers, and bibliographies that contain minimal annotation. Does not contain extensive analysis.

- CONTRACTOR REPORT. Scientific and technical findings by NASA-sponsored contractors and grantees.

- CONFERENCE PUBLICATION. Collected papers from scientific and technical conferences, symposia, seminars, or other meetings sponsored or co-sponsored by NASA.

- SPECIAL PUBLICATION. Scientific, technical, or historical information from NASA programs, projects, and missions, often concerned with subjects having substantial public interest.

- TECHNICAL TRANSLATION. English-language translations of foreign scientific and technical material pertinent to NASA's mission.

Specialized services also include organizing and publishing research results, distributing specialized research announcements and feeds, providing information desk and personal search support, and enabling data exchange services.

For more information about the NASA STI program, see the following:

- Access the NASA STI program home page at http://www.sti.nasa.gov

- Help desk contact information:

https://www.sti.nasa.gov/sti-contact-form/
and select the "General" help request type.

NASA/TM—20250002872

Single-Event Effects Test Report Texas Instruments TDA4VM System on Chip

Edward J. Wyrwas
Science Systems and Applications, Inc., Lanham MD

Scott D. Stansberry
Science Systems and Applications, Inc., Lanham MD

Test Date: 2/9/2025
Report Date: 3/19/2025

National Aeronautics and
Space Administration

Goddard Space Flight Center
Greenbelt, MD 20771

February 2025

Acknowledgments (optional)

This work was sponsored by the NASA Electronic Parts and Packaging (NEPP) Program.

Level of Review: This material has been technically reviewed by technical management.

Available from

NASA STI Program
Mail Stop 148
NASA's Langley Research Center
Hampton, VA 23681-2199

National Technical Information Service
5285 Port Royal Road
Springfield, VA 22161
703-605-6000

This report is available in electronic form at
https:// nepp.nasa.gov/

1. Introduction and Purpose

This report discusses the failure modes and heavy ion radiation sensitivity of the Texas Instruments Jacinto TDA4VM system on chip (SoC). The device was monitored for destructive events, unexpected current draw, and graphical display errors during exposure to a heavy ion beam at Lawrence Berkeley National Laboratory (LBNL)'s 88-inch cyclotron.

The purpose of the test was to determine the viability of using the TI AD4VM for general compute and its ability to render a high definition (1080p) display in space environments. The test was used to determine the effects of an operating system configuration representing different applications baselined for satellites and human-centric flight systems such as a display on a space suit or exploration vehicle with human-machine interfaces (HMI) that contain displays.

2. Test Result Summary

The TI TDA4VM system on chip did not experience any destructive events up to a LET of ~55 $MeVcm^2/mg$. While some system instability and single event functional interrupts were noted, the device operated nominally throughout the test.

3. Device Description

The device is a 16-nm FinFET System on Chip (SoC) with an ARM core complex containing two Cortex A72, six Cortex R5F, an 8-TOPS Ai accelerator and two DSP cores. The BeagleBone AI-64 (BBAI-64) single board computer (Figure 1), which acts as the test vehicle, has 4GB RAM, 16GB of flash storage, three USB 3.0 ports, an M.2 E-Key socket with PCIe, USB and SDIO, plus expansion headers providing GPIO, PWM and ADC capabilities. The device also contains a low power embedded Imagination® PowerVR® Rogue 8XE GE8430 GPU (up to 750MHz, 96GFLOPS, 6Gpix/sec) with a mini-DisplayPort display connector. The GPU is the primary point of study for this test campaign.

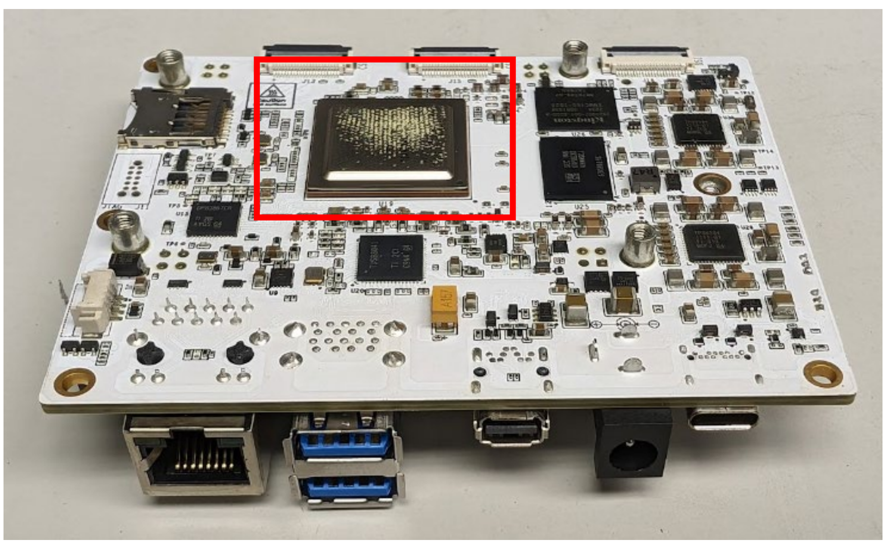

Figure 1: Photograph of BBAI-64 Single Board Computer with TI TDA4VM processor (marked)

The TI device, while low power, is capable of driving HD displays, performing H.264/H.265 encoding, inferring upon Ai models using common frameworks, and rendering 3D graphics using OpenGL and modern graphics engines (i.e., Vulkan).

It is automotive grade targeting Functional Safety-Compliance with a level of ASIL-D. The device can be procured as AEC-Q100 qualification. The device also contains embedded hardware security modules and cryptography accelerators. The memory subsystem[1] is as follows:

- Up to 8MB of on-chip L3 RAM with ECC and coherency
  - ECC error protection
  - Shared coherent cache
  - Supports internal DMA engine
- External Memory Interface (EMIF) module with ECC
  - Supports LPDDR4 memory types
  - Supports speeds up to 4266MT/s
  - 32-bit data bus with inline ECC
- General-Purpose Memory Controller (GPMC)
- 512KB on-chip SRAM in MAIN domain, protected by ECC

This device can be procured as a piece-part (24 mm × 24 mm, 0.8-mm pitch, 827-pin FCBGA, enables IPC class 3 PCB routing) or as a system-on-module permitting system designers great flexibility when it comes to system design complexity and ease of integration.

Table 1: Test and Part Information

Generic Part Number	TDA4VM
REAG ID	24-009
Manufacturer	Texas Instruments
Lot/Date Code	N/A, Procurement Q1 2024
Quantity Tested	1
Part Function	System on Chip
Package Style	24 mm × 24 mm, 0.8-mm pitch, 827-pin FCBGA
Test Engineer	Edward Wyrwas
Test Equipment	NEPP GPU Test Bench

4. Test Setup

To prepare the device for test, the TI TDA4VM was thinned to approximately 100 microns by Sage Analytical Labs. An image of the thinned die and depth map taken by Sage Analytical can be seen in Figure 2 and Figure 3, respectively.

[1] Datasheet for Texas Instruments TDA4VM Processors

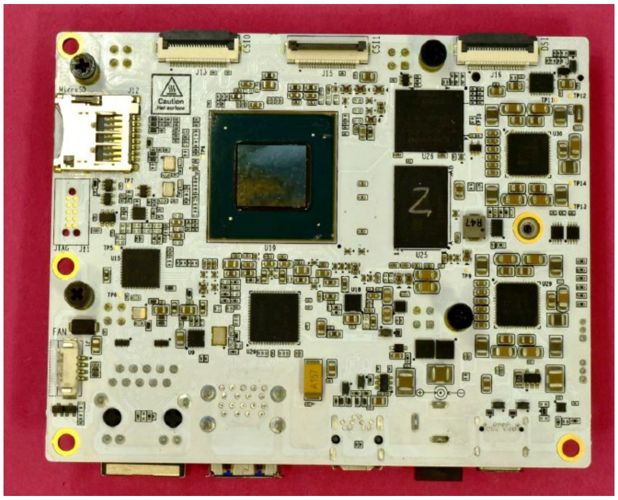

Figure 2: Photograph of Thinned TI TDA4VM Die

Figure 3: Thinned TI TDA4VM die depth map measured by Sage Analytical

5. Test Facility

This heavy ion test was performed at Lawrence Berkeley Nations Laboratory's 88-inch cyclotron. The beam tune used in the test was the 20 MeV/amu tune. The ions used in this study and the total approximate range for each is shown in Table 1.

Table 2: 20MeV/amu Ions Used in this Study

20MeV/amu Order	Ion	Symbol	Approx. LET ($MeVcm^2/mg$)	Ion Range (um)	Total Range (cm)
1	Aluminum	Al	4	380	1.038
2	Chlorine	Cl	6	310	1.031
5	Vanadium	V	13	230	1.023
3	Krypton	Kr	35	150	1.015
4	Silver	Ag	55	130	1.013

6. Test Conditions

The test was performed in-air, at an approximate distance of 1cm away from the beam's exit from its vacuum. The device was mounted at an incidence angle of 0° between the beam path and device. The device was operated nominally using a 5V 4-amp power supply. The spot size was $1cm^2$. Forced air (dry N_2) cooling was employed during the test to assure the device stayed within nominal operational conditions without a heat sink directly on top of the SoC.

7. Test Methods and Procedures

The test bench for this device is the evolution of [2, 3, 4] which permits NASA to explore more than the memory cache architecture of the device. Prior testing performed by the Aerospace Corporation [5] showed that the device was capable of performing Ai workflows and running Ai models during irradiation. Ai models were not included in the test suite for this work to best optimize the use of beam time at the facility.

The test suite operations utilized in this work consisted of the following list. The two Operating Systems (OS) allow us to compare different conditions of "Idle state" to determine if lack of a constant cache eviction routine (whether trivial or prognostics) will induce a higher cross section than running a simple operation such as one of the operational payloads (i.e., mathematics). It is worth noting that the operating system provided with the single board computer is Debian 11.3 with XFCE desktop environment.

- Debian Release 12 OS configured with Xfce desktop environment ("GPIO-OS")
- Debian 12.7 OS configured with Xfce desktop environment ("OpenGL-OS", "Pre-built Image")
- SSH remote terminal over LAN networking
- Memory Cache test with UDP packet Heartbeat monitoring
- OpenGL Rendering with real time screen capture

A replacement top side heatsink was fabricated with a window to expose the device to the beam while providing heat sinking around its perimeter. A thermal interface material was used to both assure active components could maintain vertical contact to the heatsink and also act as a shield for the micro-SD Card against scattered particles. A photograph of the mounted device can be seen in Figure 4.

The device was operated nominally using a 5V 4-amp power supply which was controlled through a relay-driven power switch in the operator room. The other equipment in the cave was connected to a network-controlled power switch for remote operation and troubleshooting to minimize downtime. The voltage, current and power was monitored in-situ using a microcontroller with sensors for the same. This monitoring system also provided in-cave environmental readings of humidity, temperature, and atmospheric pressure. This monitoring system was connected to the Wireless network in the cave.

This device monitoring system also provided a rigid mounting point for the BBAI-64 through a set of stacked headers on its GPIO. A 3D printed fixture was created to mount this PCBA to the motion control system in the cave for consistent placement of the device if more than one device was to be tested (in case of destructive failure).

---

[2] Considerations for GPU SEE Testing. E. Wyrwas. NASA 2017. https://ntrs.nasa.gov/citations/20170004734

[3] Standardizing Microprocessor and GPU Radiation Test Approaches. E. Wyrwas. NASA 2019. https://ntrs.nasa.gov/api/citations/20190028690/downloads/20190028690.pdf

[4] AMD Radeon e9173 Low Power PCIE GPU Single Event Effects Test Report. E. Wyrwas. NASA 2023. https://ntrs.nasa.gov/citations/20230009291

[5] Proton Testing of Texas Instruments TDA4VM SoC. S. Davis. IEEE NSREC 2024. https://ieeexplore.ieee.org/document/10759193

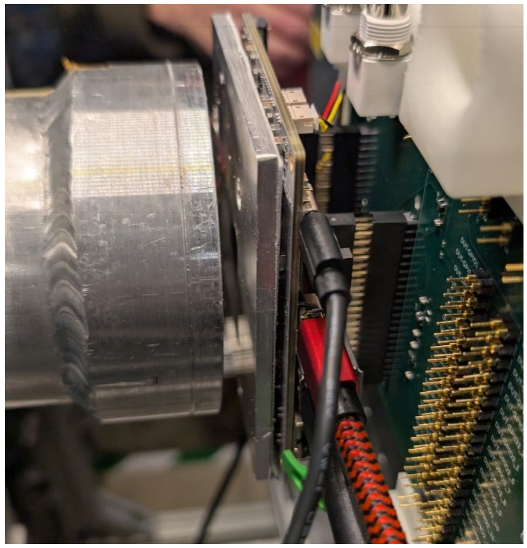

Figure 4: Photograph of BBAI-64 PCBA Mounting

The monitoring data was recorded to a time-series database called InfluxDB[6] and monitored using a Grafana[7] dashboard. An example of this dashboard is shown in Figure 5. The TI AD4VM device's GPU was monitored in real time using Open Broadcast Studio[8] (OBS) and a high-definition GPU Capture device connected to a Windows laptop. A notional diagram of the test bench is shown in Figure 6 and Figure 7.

Figure 5: Exemplar Grafana Dashboard showing Current Draw at Different Modes of Operation
(Red – Single Event Functional Interrupt, Yellow 1 - Power Cycle, Blue- Boot Process, Green - Idle Operation, Yellow 2 – Power Off)

[6] https://www.influxdata.com/
[7] https://grafana.com/
[8] https://obsproject.com/

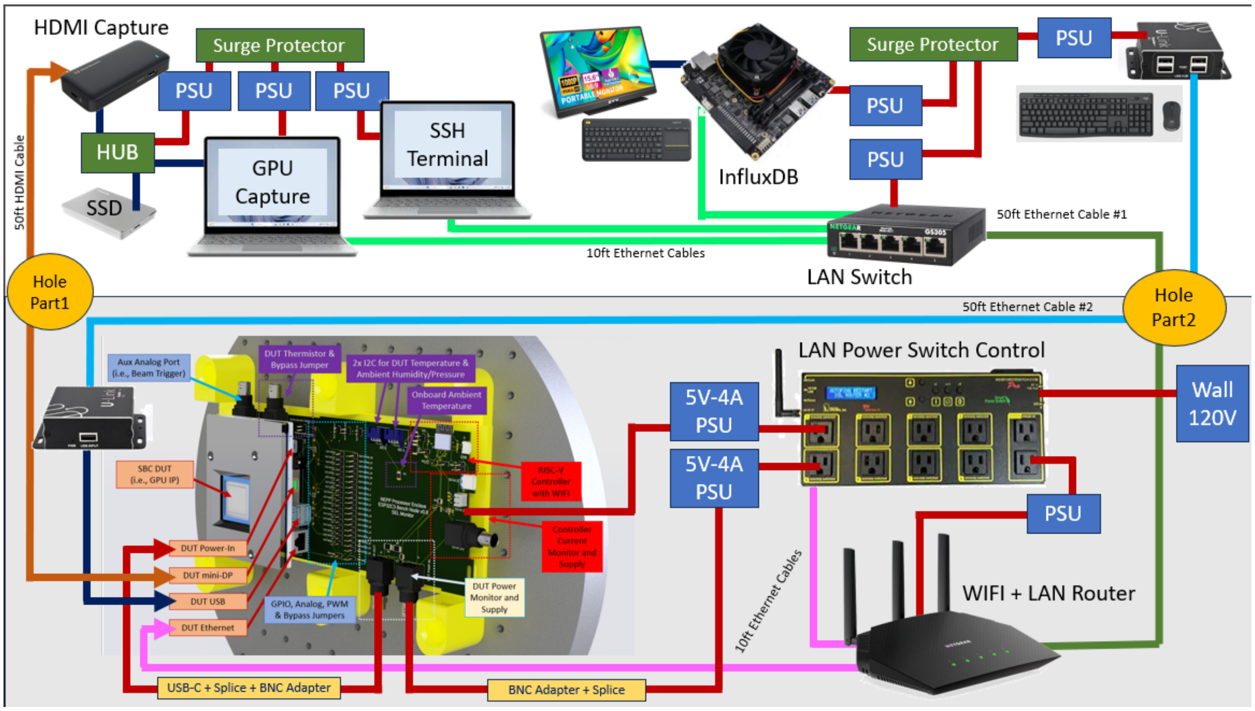

Figure 6: Diagram of Test Bench Configuration

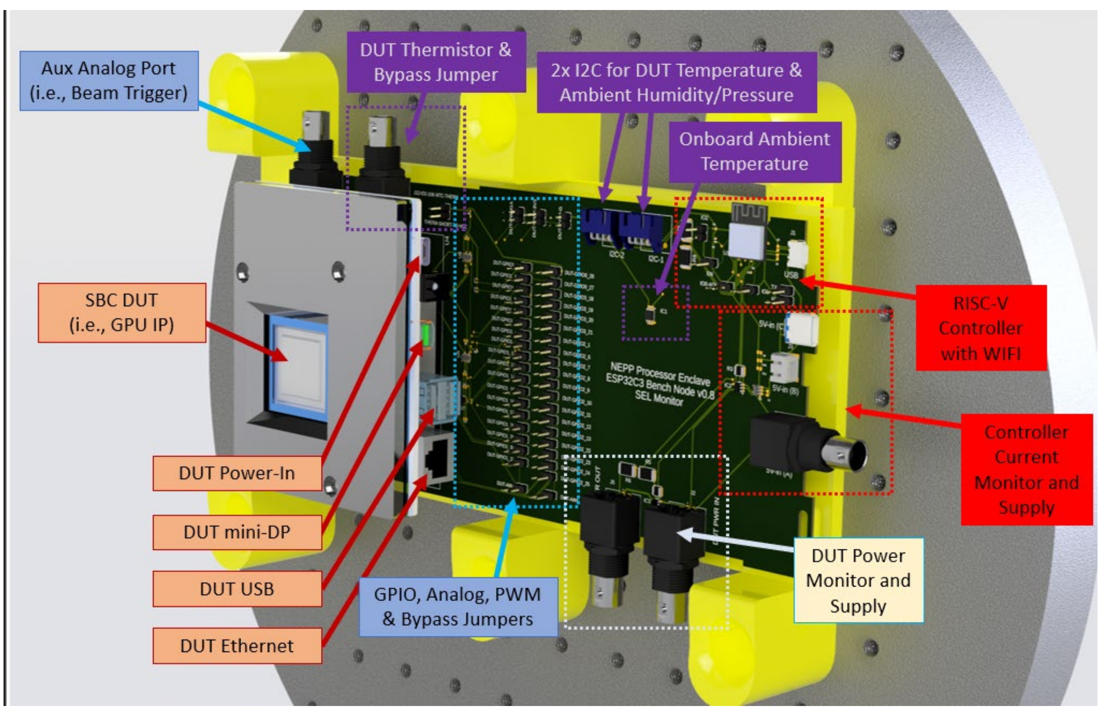

Figure 7: Diagram of BBAI-64 Mounting Configuration

The graphics display was recorded and saved to file for post processing of individual frames to identify and quantify pixel defects and erroneous operation. An exemplar screenshot showing the recording of the GPU rendering test, test script operation and environmental monitoring as seen during the test is provided in Figure 8. The post processing utilized the FFMPEG[9] applications and Python's OpenCV[10] library to convert the video files into individual frames, and then compare sequential frames for red, green, and blue channel defects. The quantity of defects for each channel was recorded to a spreadsheet along with the frame number associated with it. The frames were extracted at 1 frame per second which permitted a secondary metric to assess the approximate time to failure versus what was recorded in the electrical monitoring system.

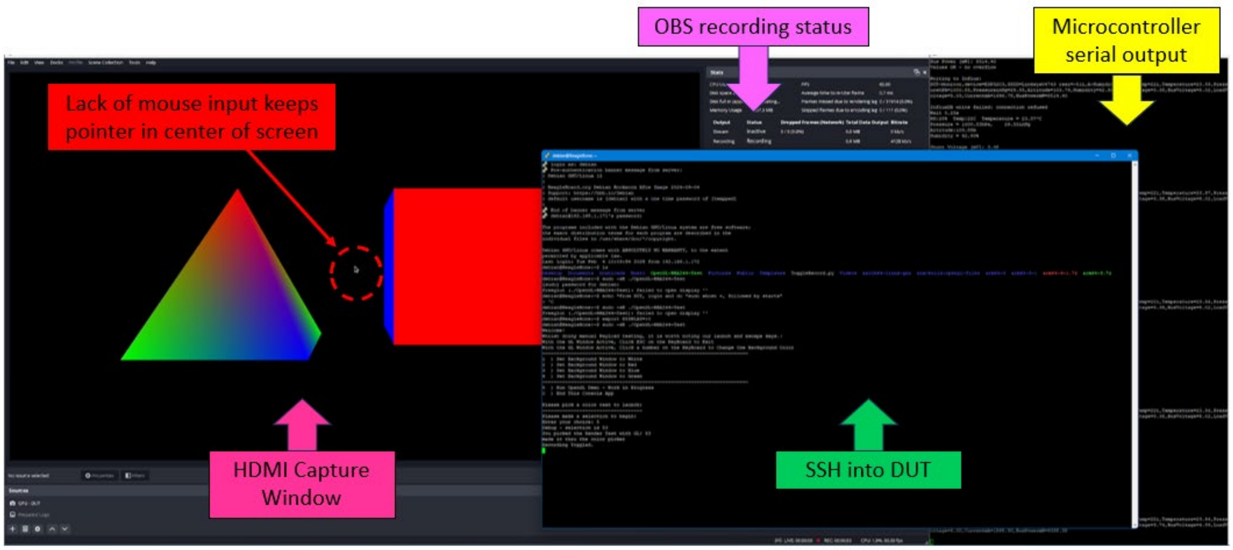

Figure 8: GPU Monitoring Setup using OBS

The UDP test was executed using a Raspberry Pi 4b connected to the BBAI64's UART port. All output from the UART was saved into a log file for post processing of operating system errors and other single event functional interrupts (SEFI). These errors were tabulated, and a high-level diagnostic was performed to determine the underlying cause, if one was reported by the operating system kernel or its watchdog routines[11]. Each ARM64 core produced its own UDP heartbeat traffic so that the UDP listener could also produce a log showing any divergence of timing between the cores or whether one or both cores failed to produce a heartbeat.

[9] https://www.ffmpeg.org/
[10] https://docs.opencv.org/4.x/d6/d00/tutorial_py_root.html
[11] https://patchwork.kernel.org/project/linux-arm-kernel/patch/1540512876-12011-1-git-send-email-sudaraja@codeaurora.org/

The OpenGL rendering test was executed by a second Raspberry Pi 4b on the test bench network connected to the BBAI-64 by secure shell (SSH) using a terminal. This test launched the graphics window on the BBAI-64's display which was subsequently captured by OBS. As with the UDP test, the device's system logs were saved to the Raspberry Pi connected to the UART port.

8. Test Results

Failures of either test instituted an immediate power-off and power-cycle of the device. Failure is also defined as current draw either less than or greater than what was expected during nominal operation (no-beam applied) for the given test routine. This became a clear indication that a latch-up event took place causing system failure or instability. A total of 69 test runs were completed. The majority of the test runs ended in a SEFI failure and were used to assess the radiation response via cross section metric for the device. The data for each operating system configuration was binned as well as the total response for the device. The SEFI cross section for each Linear Energy Transfer (LET) (MeV cm^2/mg) is shown in Figure 9.

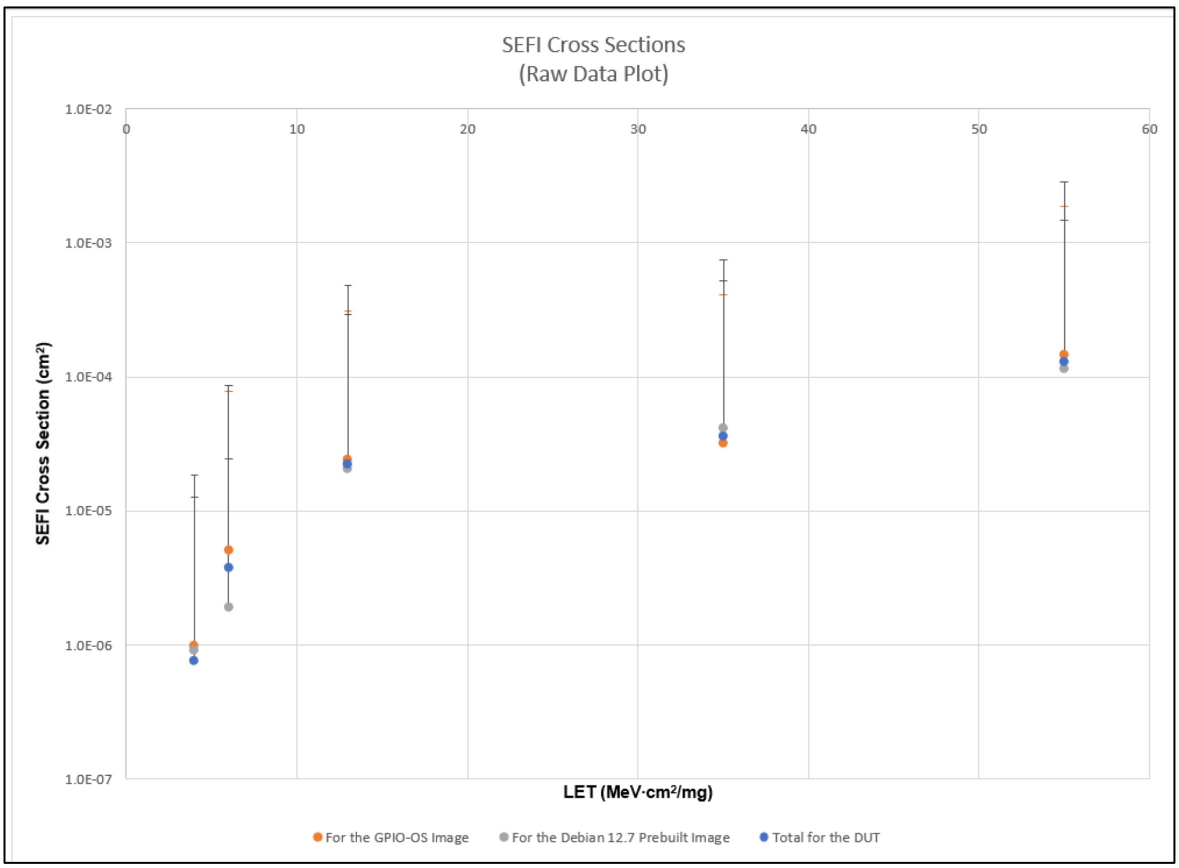

Figure 9: SEFI Cross Sections for the GPIO-OS, Pre-built Image, and Total Device with Poisson 95% confidence intervals

The results of this test show that the TI TDA4VM system on chip can operate in a space environment if an electrical monitoring system is present. All effects seen either forced the system to reset on its own or had a notable difference in actual current draw versus what was expected during the mode of operation of the device under test. This device aligns well with other microprocessor tests [4, 12, 13, 14] saturating at a cross section approximately 1E-4 cm^2.

Table 3: Weibull Parameters for this Heavy Ion Test - TI TDA4VM SoC

Model Parameter	**Fitted Value**
Onset LET	4 MeV cm^2/mg
Saturated Cross Section	1.3022E-04 cm^2
Shape	0.84873
Width	0.999995 MeV cm^2/mg

[12] EdgeCortix SAKURA-I Machine-Learning, PCIe Accelerator SEE Heavy Ion Test Report. S. Roffe. NASA 2024. https://ntrs.nasa.gov/citations/20240015800
[13] Recent Radiation Test Results on COTS AI Edge Processing ASICs. M. Casey. NASA 2022. https://ntrs.nasa.gov/citations/20220009215
[14] Proton and Heavy Ion SEE Data on NVIDIA and AMD GPUs. M. Cannon. IEEE NSREC 2023. https://ieeexplore.ieee.org/document/10265847

9. Appendix

The following figures show the different types of errors recorded for the GPU during UDP test as well as the GPU rendering test versus the expected display output. Screenshots containing red circles were extracted from the pixel defect analysis.

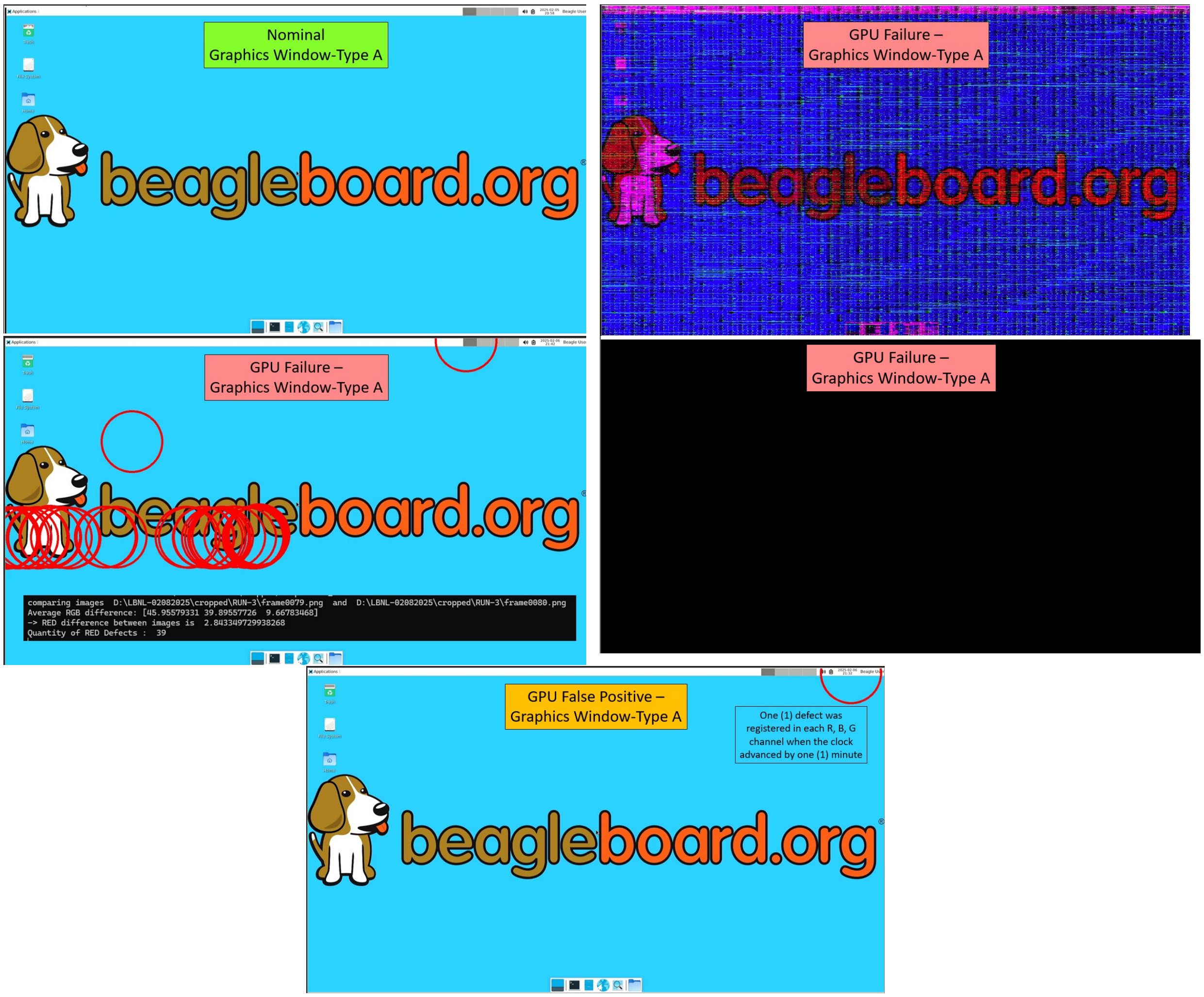

Figure 10: GPU Error Signatures for UDP Test

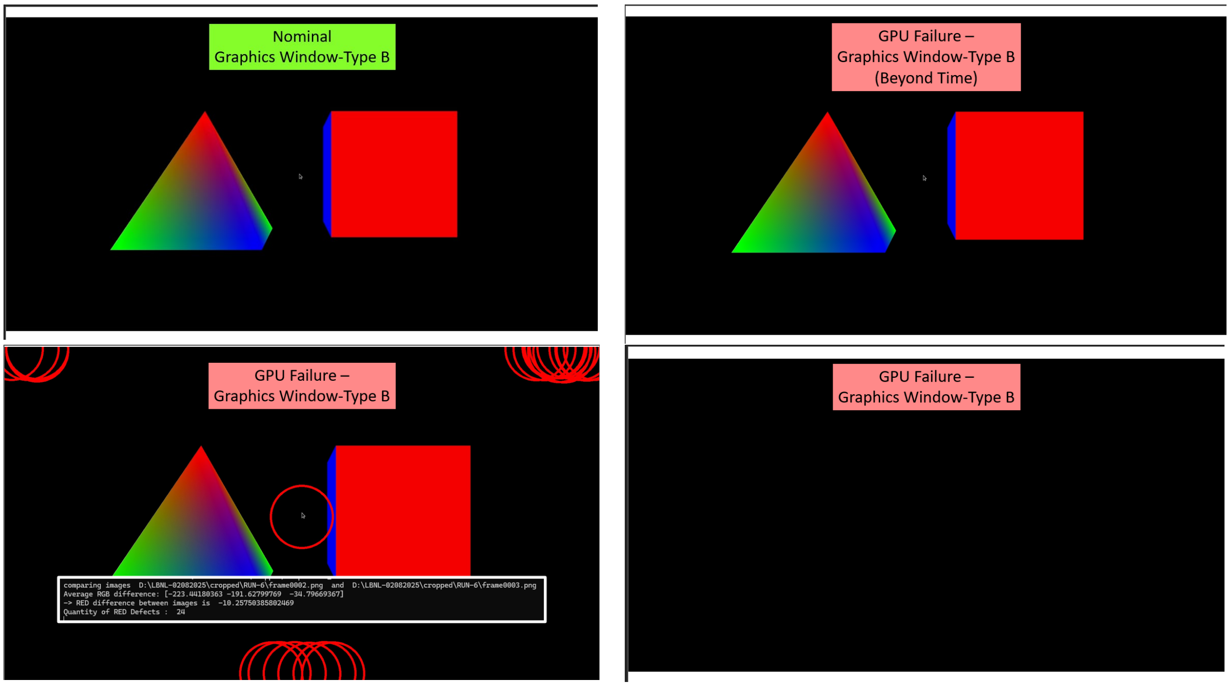

Figure 11: GPU Error Signatures for Graphics Rendering Test

The data from the InfluxDB was exported for assessment using Python and interactive plots so that individual test runs, and smaller time window sampling could be focused on. The following figures show two levels of electrical instability which are indicative of latch-up events. The modes of operation are indicated as well as the region of the comparison for the data in the plots.

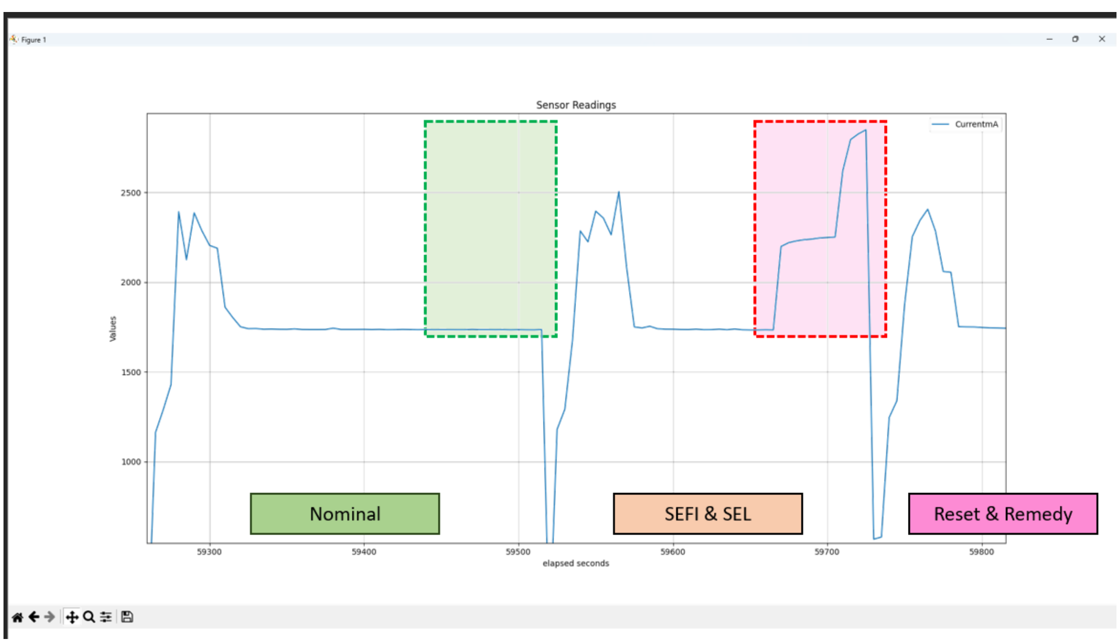

Figure 12: Large Electrical Anomaly indicating Single Event Latch-up and Single Event Functional Interrupt

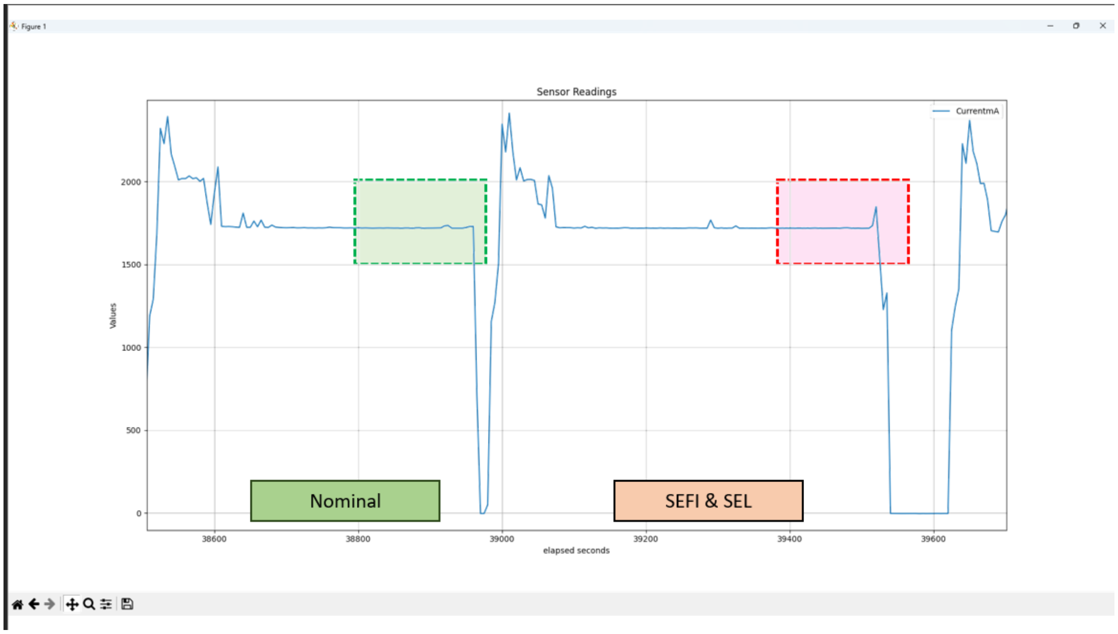

Figure 13: Small Electrical Anomaly indicating Single Event Latch-up and Single Event Functional Interrupt

While there was no indication that the environmental conditions in the cave caused deviation in the performance of the TI AD4VM or its test data, there was good correlation to indicate WIFI strength was impacted by the humidity and temperature in the cave. The physical location of the Wireless Router and the TI AD4VM did not change during the course of the 12-hour test and therefore are not contributors to the effects seen. Fortunately, the WIFI strength was satisfactory and did not cause any interruptions on data collection.

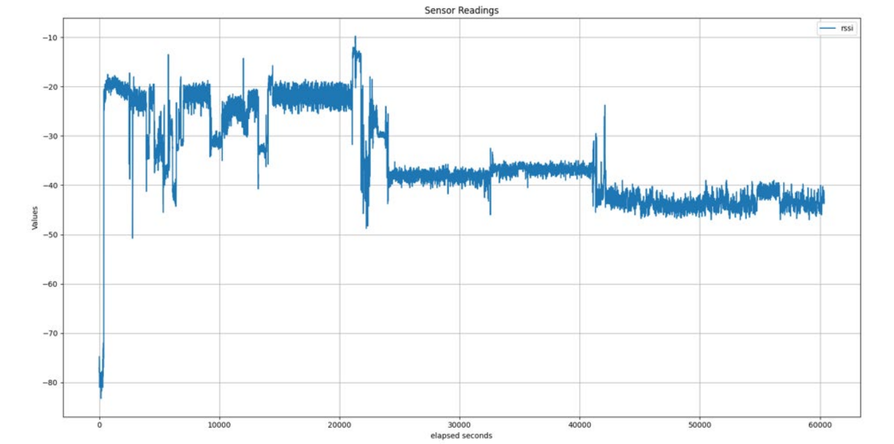

WIFI Signal Strength

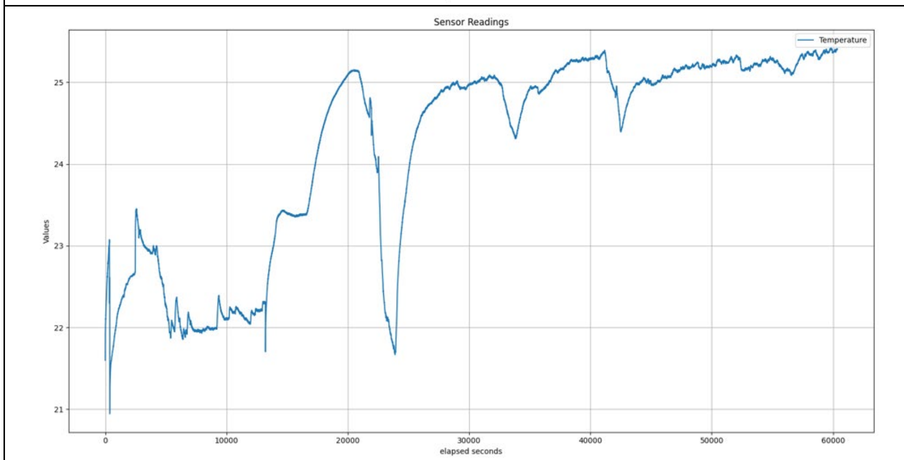

Temperature

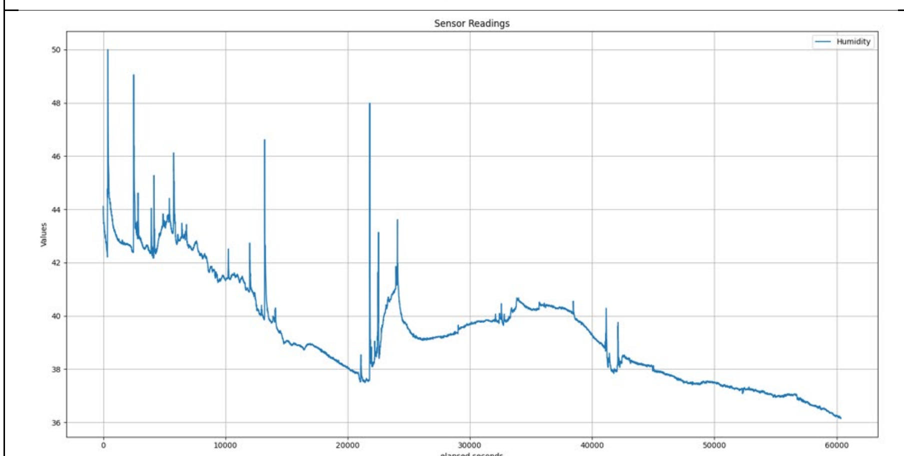

Relative Humidity

Figure 14: WIFI Strength versus Temperature and Relative Humidity during the Entire Testing Window